Carbons prepared from *Spartina alterniflora* and its anaerobically digested residue by H₃PO₄ activation: Characterization and adsorption of cadmium from aqueous solutions

Zhengfang Wang, Er Nie, Jihua Li, Yongjun Zhao, Xingzhang Luo, Zheng Zheng*

Environmental Science and Engineering Department, Fudan University, Shanghai 200433, China

ABSTRACT

Two series of activated carbons were prepared from *Spartina alterniflora* and from its anaerobically digested residue by H₃PO₄ activation at various process conditions, and used as adsorbents for the removal of cadmium (II) in aqueous solutions. The surface areas and pore volumes of carbons were derived from adsorption isotherms (N_2 at 77 K). The surface chemistry of carbons was investigated by infrared spectroscopy. Comparison study indicated that physicochemical properties of the activated carbons were strongly dependent not only on activation conditions but also on biopolymer contents of precursors. Several isotherm models were investigated and the adsorption isotherm data were best represented by the Langmuir isotherm model, with a maximum monolayer adsorption capacity of 47.85 mg/g at 25 °C. The results showed that the activated carbon produced from *S. alterniflora* could be employed as a promising adsorbent for removing cadmium (II) from aqueous solutions.

© 2011 Elsevier B.V. All rights reserved.

1. Introduction

Contamination of heavy metals in our water supplies has steadily increased over the last few years as a result of overpopulation and rapid industrialization. Cadmium is an important precursor used as an intermediate in processing industries such as smelting, Cd–Ni batteries, oil paint, mining pigments, stabilizer and alloy manufacturing [1]. However, the presence of cadmium (II) in water, even at very low concentrations, is extremely harmful to the aquatic environment and human health in terms of muscular cramps, chronic pulmonary problems, renal degradation, proteinuria, skeletal deformity, muscular cramps and testicular atrophy [2]. Therefore it has been listed as one of the priority contaminants in water for removal in many countries, including China.

Physical and chemical treatment technologies such as chemical precipitation, membrane filtration, ion exchange, carbon adsorption and coprecipitation/adsorption have been extensively studied to remove cadmium (II) from industrial wastewaters. Among these techniques, adsorption is commonly used because of its relatively easy process and high efficiency. Activated carbon has been widely used as adsorbent material due to its extensive surface area, high degree of surface reactivity, and adaptable pore size distribution. Furthermore, there are a few reports that activated carbons pre-

pared by H₃PO₄ activation exhibit remarkable cation-exchange capacities [3], which made them useful for the removal of heavy metals from aqueous solutions. Activated carbon from cheaper and readily available resources, most of which are agricultural, domestic, industrial wastes; such as olive stone [4], sawdust [5], rice hull [6], plant biomass [7], Phragmites australi [8], etc, have been successfully employed.

Spartina alterniflora, a salt marsh plant native to coastal states of the eastern and southern U.S., was introduced into China in 1979 for erosion control [9], and it has been expanding rapidly in intertidal flats of many regions of China ever since. It now covers a total area of about 112,000 ha, and is spread from Tianjin City (117.20°E, 39.13°N) in the north to Guangxi Province (109.12°E, 21.49°N) in the south [10]. The mono-dominant community of *S. alterniflora* accounted for almost one quarter of the total area of intertidal salt marshes in Shanghai by 2005 [11]. For Jiangsu Province (the total length of the coastline being 954 km), the *S. alterniflora* marshes, with a width up to more than 4 km, are distributed over a section of 410 km coastlines [10,12]. However, evidence has been recently reported that *S. alterniflora* may out-compete native plants, threaten the native ecosystems and coastal aquaculture, and cause declines in native species richness [13]. Due to its extensive invasion and replacement of native wetland vegetation, *S. alterniflora* is considered as a bioinvasive species by the State Environmental Protection Administration of China [14]. In recent years, efforts have been made to use *S. alterniflora*, such as biogas production, feeding livestock, fertilizing soils, extracting the biomineral liquid

---

* Corresponding author. Tel.: +86 21 65642948; fax: +86 21 65642948.
E-mail address: zzhenghj@fudan.edu.cn (Z. Zheng).

with a number of health functions [15], and so on. Considering its plentiful, renewable supply and favorable lignocellulosic nature [16], activated carbon production may be one promising method of using *S. alterniflora* from both multipurpose use of wastes and environmental pollution prevention.

The object of this study is to investigate the potential feasibility of activated carbon from *S. alterniflora* for the adsorption of cadmium (II). Anaerobically digested residue of *S. alterniflora* was chosen as another precursor for comparison under identical experimental conditions, since it's the same species with *S. alterniflora* but had different biopolymer contents. It was used as a reference for same type materials in assessing the viability of other materials for activated carbon production. The effects of the composition of lignocellulosic precursors and the activation conditions (the impregnation ratio between H_3PO_4 and precursors and activation temperature) on the physicochemical properties of the carbons obtained were studied. The best combination of operating conditions to prepare activated carbons for cadmium (II) adsorption was identified. The different models were applied to fit the experimental data and the equilibrium data were analyzed so that we can understand the adsorption mechanism.

2. Materials and methods

2.1. Materials used and sample preparation

S. alterniflora (SA) and anaerobically digested residue of *S. alterniflora* (ADSA) were used. SA was collected from a *S. alterniflora* plain muddy salt marsh in Yancheng city, Jiangsu Province, China. ADSA was prepared by anaerobic digestion of SA at a constant temperature of 35 °C for 60 days. At first, the precursors were washed thoroughly with water to remove foreign materials such as mud and salt, and then ground in a laboratory mill, dried at 120 °C in an oven for 24 h and sieved to a uniform particle size (120 mesh) for activation. Laboratory grade H_3PO_4 was used as activating agent. The process of preparing activated carbons from SA and ADSA can be divided into the following three stages:

(i) Acid-washing. Prior to impregnation with H_3PO_4, the precursors were washed with 1% (w/w) H_2SO_4 aqueous solution followed by deionized water at 25 °C and dried at 120 °C in an oven to 12 h.

(ii) Activation. The precursors were impregnated with H_3PO_4 and water at various ratios. The impregnation ratio (r = mass of H_3PO_4 relative to that of dried precursors) was varied from 0.5 to 3.0. The impregnated precursors were dried for 24 h at 105 °C in an oven and then heated to different activation temperatures in an electrically heated, horizontal-tube furnace with a ramp rate of 5 °C/min. Different activation temperatures within the 400–700 °C range were investigated. After reaching the preset activation temperature, the mixtures were cooled down to room temperature inside the furnace. All activation steps were carried out under N_2 atmosphere with a flow rate of 100 ml/min.

(iii) Washing and drying. After being cooled to room temperature, the activation mixtures were washed several times with hot deionized water until neutral pH. Then the sample was dried at 105 °C in an oven for 24 h. The final weight of dry sample was recorded to determine product yield (Y% = weight of activated product relative to the initial precursor weight). The losses accumulating for ADSA at the anaerobic digestion has not been taken into account. The sample was ground and sieved to a uniform particle size (200 mesh) for further measurements.

The carbon samples were identified with a SA/ADSA followed by two numbers indicating the impregnation ratio and the activation temperature (°C). Thus, the sample SA-1-500 and ADSA-1-500 correspond to the activated carbons prepared from SA and ADSA at r = 1.0 and 500 °C activation temperature, respectively.

2.2. Activated carbon characterization

Morphological characterization of the activated carbon was carried out by N_2 adsorption at 77 K using a Micrometritics ASAP-2020 Surface Analyzer in the relative pressure range of 0.01–1. The Brunauer–Emmett–Teller (BET) surface areas (S_{BET}) were calculated from the N_2 adsorption isotherms using the BET equation [17]; micropore volume (V_{mi}) and micropore specific surface area (S_{mi}) were obtained using the *t-plots* method [18]; mesopore volume (V_{meso}) and mesopore specific surface area (S_{meso}) were determined by the Barrett–Joyner–Halenda (BJH) model. The total pore volume (V_T) was obtained from the amount of nitrogen adsorbed at a relative pressure around 0.98. A batch equilibrium method for determination of the point of zero charge (pH_{PZC}) was proposed by one of the authors [19].

The surface functional groups of samples were identified by transmission infrared spectra obtained from a Fourier transform spectrophotometer (Nicolet Model Nexus 870, USA) using pellets of KBr containing about 0.5% finely ground activated carbon samples. These pellets were dried overnight at 120 °C before the spectra were recorded and the spectra were the result of averaging 60 scans with a spectral resolution of 2 cm^{-1} with the range of 400–4000 cm^{-1}.

2.3. Adsorption experiments

All cadmium cation stock solutions were prepared from $Cd(NO_3)_2$ (Nanjing Chemical Reagent Co., China) at a concentration of 1000 mg/L. Experimental solutions at the desired concentration were then obtained by successive dilutions. In the batch studies, the adsorption experiments were carried out by adding 0.1 g of activated carbon to 100 ml of $Cd(NO_3)_2$ solutions at known concentration (5–100 mg/L) and pH (2–10) in a 250 ml stoppered bottles placed in a thermostated shaker for 24 h at 25 °C. At the end of each step, the supernatant liquids were filtered and the residual cadmium concentrations were measured by atomic absorption spectrophotometer (SOLAAR M6, Thermo) at 228.8 nm wavelength. The amount of metal ion adsorbed per unit mass of adsorbent at equilibrium (q_e) was calculated using the following equation: $q_e = (C_0 - C_e) V/W$, where C_0 and C_e are the initial and equilibrium liquid-phase concentrations of metal ions, respectively (mg/L); V is the volume of the solution (L), and W is the mass of the adsorbent (g).

3. Results and discussion

The results of proximate/ultimate analyses and biopolymer content determination for precursors are given in Table 1. It can be found that both precursors are typical lignocellulosic materials, and the cellulose, hemicelluloses and lignin contents account for 74.37% and 78.70% for SA and ADSA's gross quantity, respectively. The ash content of both precursors is similar; however, they differ in biopolymer composition. The relative content of lignin in SA increased compared with that of cellulose and hemicelluloses after anaerobic digestion [20]. Compared to SA, ADSA contains much higher amount of lignin and slightly lower amount of cellulose and hemicelluloses. It is known that the biopolymer composition of precursors has an essential influence on the product yield [21], the development of porosity [22] and also the surface functional groups of samples [23].

Table 1
Composition of precursors used.

	SA	ADSA
Ash (db, wt%)	6.78	6.35
Ultimate analysis (db, wt%)		
C	46.70	49.22
H	6.10	6.49
O	42.30	37.36
N	0.15	0.59
Biopolymer content (wt%)		
Cellulose	38.00	35.00
Hemicellulose	27.20	20.00
Lignin	9.17	23.70

3.1. Product yield of the activated carbons

Product yield is an important parameter of the feasibility of preparing activated carbon from a given precursor. The yield values of SA fall within a relatively narrow range of 41.85–45.50%. Results indicate that at fixed activation temperature, the product yield of ADSA is nearly 10–15% higher than SA. This difference could be attributed to the lignocellulosic composition of the materials as it is commonly accepted that the product yield depends on the content of lignin [21]. Higher lignin content results in higher char yield.

3.2. Characterization of the activated carbons

3.2.1. Surface area and pore structural characterization analysis of the activated carbons

3.2.1.1. The effect of impregnation ratio between H_3PO_4 and precursor. A comparison result of pore structure characterization obtained from nitrogen adsorption isotherms for samples prepared from SA and ADSA at 500 °C is shown as a function of impregnation ratio in Fig. 1. It clearly shows that the impregnation ratio affects significantly on the surface area and pore volume. The BET surface areas of carbons produced from SA and ADSA reached a maximum at an impregnation ratio of approximately 1.0 and 2.0, respectively. Further increases in impregnation ratio, resulted in a decrease in the BET surface area of carbons (Fig. 1a). A similar trend is observed for the mesopore S_{meso} while the mesopore surface area from ADSA increased rapidly, and then showed a decrease trend. For carbons from SA, the micropore specific surface area decreased across the entire range of impregnation ratio explored in this study; while that of carbons from ADSA increased slightly, and then decreased obviously.

As shown in Fig. 1b, with the increasing impregnation ratio, both total and mesopore volumes of the activated carbons from SA increase while the volumes of microporosity decrease considerably. This can be attributed to the intensified structure dilation which appears to occur as larger amount of acid is incorporated into the SA resulting in widening the existing pores [24]. However, for the carbons from ADSA, both total and mesopore volume reached a maximum at an impregnation ratio of approximately 2.0, and then decreased. Moreover, at any impregnation ratio, the total and mesopore volume in SA is always higher than the amount in ADSA, and the difference is more pronounced at higher impregnation ratio. This observation could be explained by the different reactivity when the precursors with different biopolymer compositions are subjected to acidic conditions.

Experimental results suggest that both biopolymer composition of precursor and impregnation ratio can be used as independent variables in the control of the porosity of carbon products.

3.2.1.2. The effect of activation temperature. The surface areas and pore volumes of carbons produced at different activation temperatures using an impregnation ratio of 1.0 are summarized in Fig. 2.
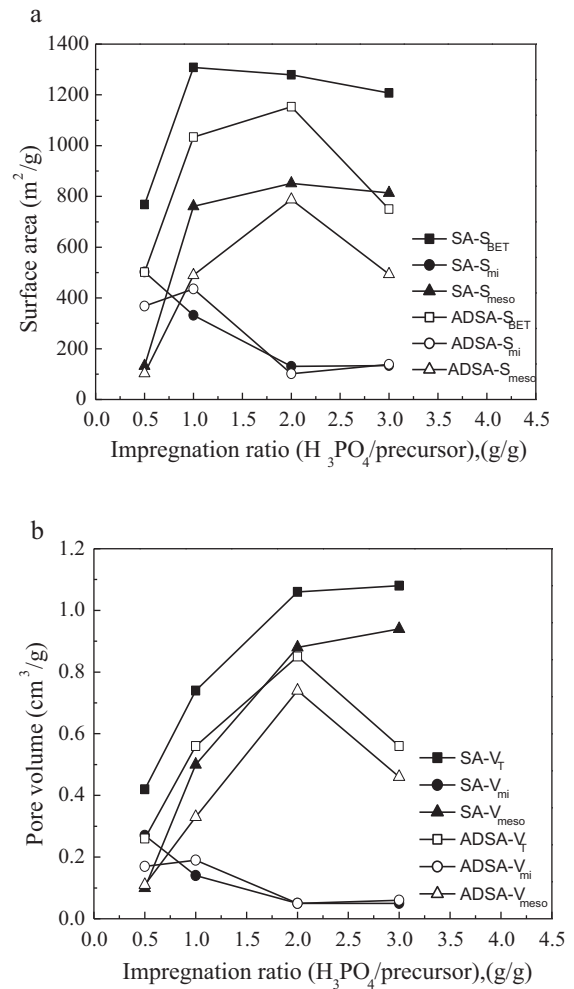

Fig. 1. Effect of impregnation ratio on surface area (a) and pore structure (b) of carbons produced from SA and ADSA by H_3PO_4 activation at activation temperature 500 °C.

Activation proceeds at relatively low temperature, with a considerable development of BET surface area. Especially, for carbons from SA (Fig. 2a), the maximum surface area more than 1339 m^2/g at an impregnation ratio of 1.0 reached at 400 °C. With increasing carbonization temperature from 400 to 700 °C, the BET surface area and total pore volume decrease. For carbons from ADSA, the BET surface area reaches a maximum value close to 1152 m^2/g at around 500 °C and then decreases slowly with further increase in activation temperature. These same results were reported by other researchers [25], suggesting that during the chemical activation of lignocellulosic precursors, the phosphoric acid forms phosphate and polyphosphate bridges that connect the biopolymer fragments avoiding contraction of the material by the effects of the temperature. These phosphate and polyphosphate bridges are thermally unstable above 450 °C, leading to a decrease in porosity by contraction of the char. Compared to SA, the ADSA is characterized by slightly lower content of cellulose and considerable higher content of lignin. The activated carbons prepared from SA are more mesoporous in their nature than those from ADSA across the entire activation temperature range investigated in this study, indicating that cellulose is responsible for the development of mesoporosity [26]. At activation temperatures above 500 °C, the micropore volume of carbon from ADSA was little higher than that of carbon from the SA with relatively lower lignin content (Fig. 2b). This can result from the higher content of lignin in ADSA [23]. Thus, a significant
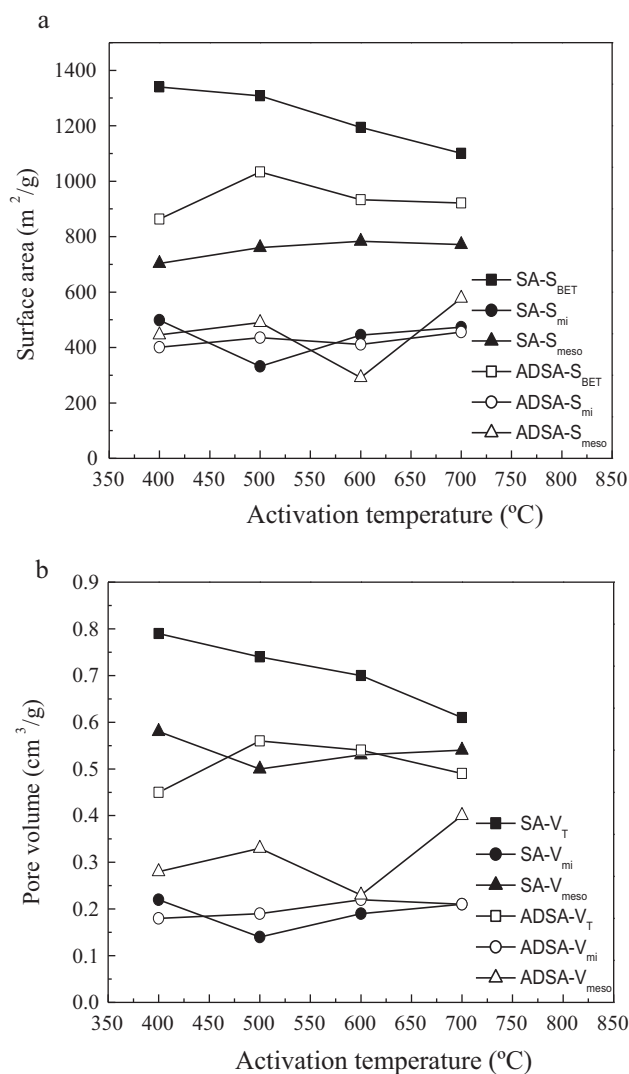
Fig. 2. Effect of activation temperature on surface area (a) and pore structure (b) of carbons produced from SA and ADSA by H_3PO_4 activation at impregnation ratio of 1.0.

effect of the activation temperature on the porous structure for activated carbons is obvious. In addition, under the same preparation conditions, the precursor with different biopolymer compositions will affect both surface area and pore volume.

3.2.2. Functional group analysis of the activated carbons
3.2.2.1. The effect of impregnation ratio.
FTIR spectra of carbon products prepared from SA and ADSA with different impregnation ratios at 500 °C are illustrated in Fig. 3. All the spectra exhibit a strong band at 1570 cm^{-1} due to combined stretching vibrations of conjugated C=O group and aromatic rings [25]. The carbon obtained across the entire impregnation ratio range investigated in this study shows a small peak at 1710 cm^{-1} characteristic of the C=O stretching vibration in ketones, aldehydes, lactones and carboxyl groups [23]. The small intensity of this peak suggests a relatively low content of carboxylic groups as compared to other oxygen groups of carbon adsorbents. The strong bands located around 1170 cm^{-1} can be attributed to the stretching vibration of hydrogen-bonded P=O groups from phosphates or polyphosphates, the O–C stretching vibration in the P–O–C$_{(aromatic)}$ linkage, and P=OOH [25]. With an increase in impregnation ratio from 1.0 to 3.0, the relative intensity at band 1170 cm^{-1} increases. This indicates the density change of phosphorus-containing groups.
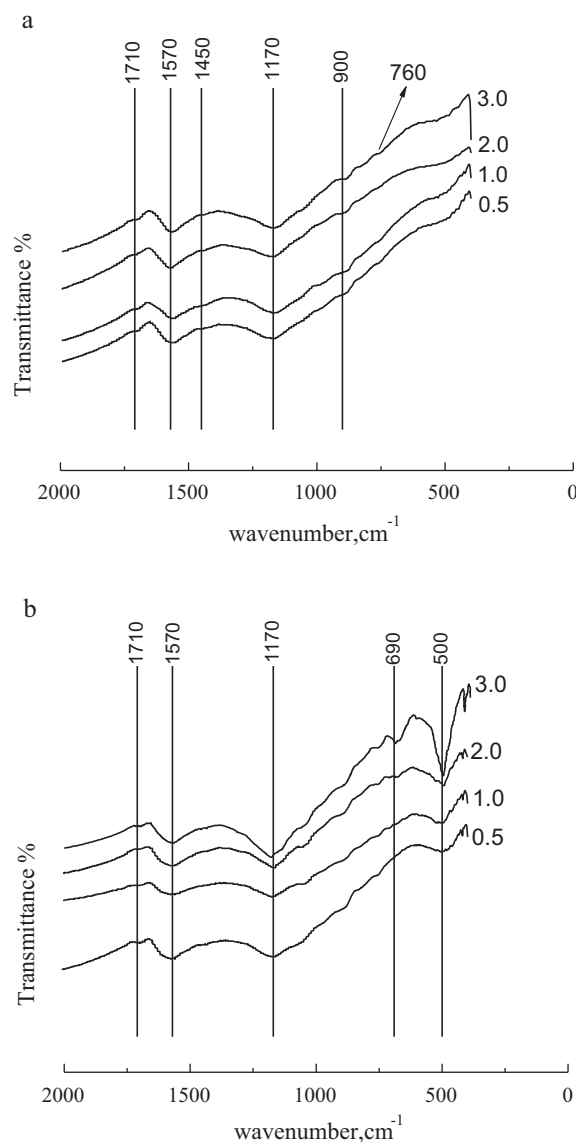

Fig. 3. FTIR spectra of carbons prepared from SA (a) and ADSA (b) with different impregnation ratios at activation temperature 500 °C.

For carbons prepared from SA (Fig. 3a) at the impregnation ratios of 0.5 and 1.0, similar FTIR spectra were obtained. The FTIR spectra of carbons show small changes at 1710 cm^{-1} band and 1570 cm^{-1} band with different impregnation ratios. This indicates that C=O band of diketones, keto-esters, keto-enol structures did not change much at different impregnation ratios [27]. The band around 1450 cm^{-1} can be attributed to C–H stretch. Increase in the impregnation ratio does not have an apparent impact on the formation of related groups. When impregnation ratio is increased from 1.0 to 3.0, the band around 900 cm^{-1} together with 760 cm^{-1} appears, which could be attributed to a increase in phosphorous-containing groups [28]. As shown in Fig. 3b, the relative intensity of band at 1710 cm^{-1} attributed to carbonyl groups is weak, demonstrating that the content of carboxylic groups and other carbonyl-containing groups is low. Overall, the spectra indicate that the relative intensity band around 1170 cm^{-1} caused by phosphorus-containing groups is higher compared to that of band contributed by carbonyl groups (1710 cm^{-1}), and its functionality with impregnation ratio is clear.

Comparing the FTIR spectra of carbons from different precursors at the same impregnation ratio, one of the most significant
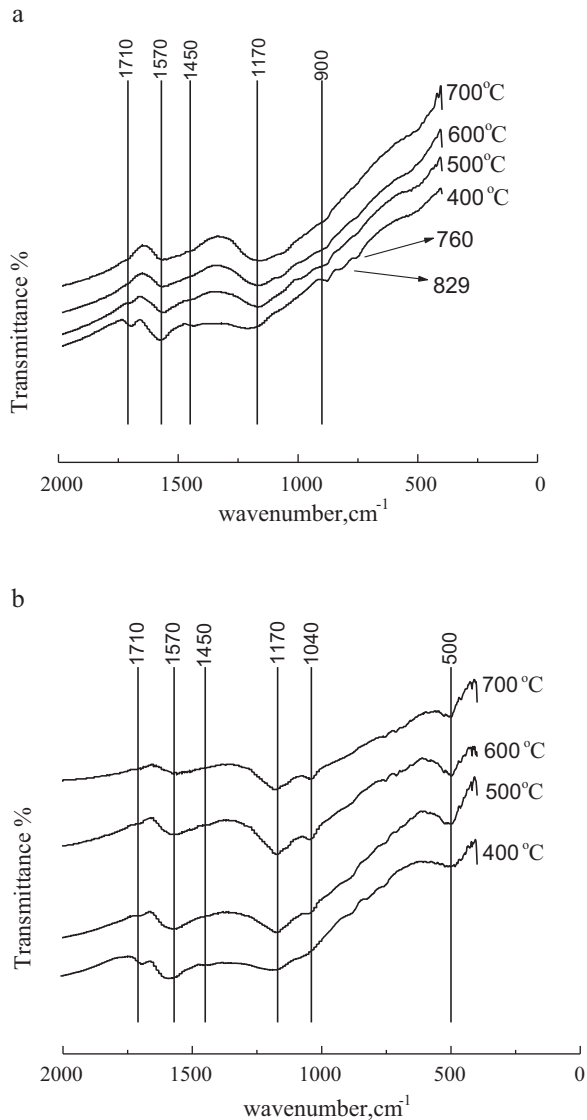
Fig. 4. FTIR spectra of carbons prepared from SA (a) and ADSA (b) at different activation temperatures with impregnation ratio of 1.0.
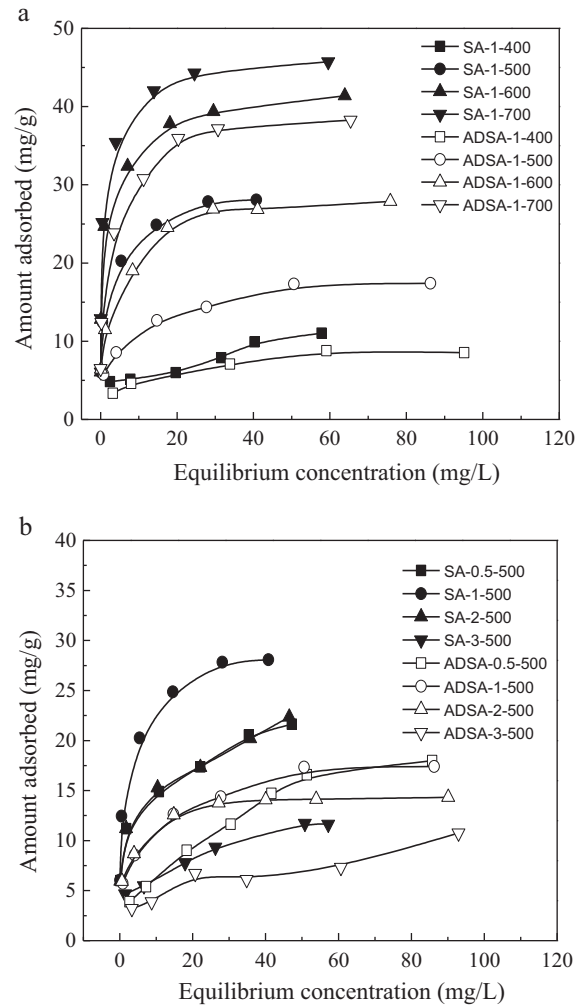

Fig. 5. Adsorption isotherms of cadmium (II) (25 °C) on carbons prepared from SA and ADSA at different activation temperatures (a) and different impregnation ratios (b).

differences observed in the spectra of carbons prepared from SA and ADSA was the relative intensity of band around $500\,\text{cm}^{-1}$ together with $1170\,\text{cm}^{-1}$ caused by phosphorus-containing groups. It can be seen that the formation of phosphorus-containing groups occurs much more readily on activated carbons from ADSA than SA. This demonstrates the critical effect of precursor on the surface chemistry properties of carbon products. The FTIR spectra of carbons prepared with different impregnation ratios also indicates that higher impregnation ratio aids in the formation of phosphorus-containing groups.

3.2.2.2. The effect of activation temperature. FTIR analysis results of carbons prepared from SA and ADSA with an impregnation ratio of 1.0 at various activation temperatures are give in Fig. 4. With an increase of activation temperature to 700 °C, the FTIR spectra of carbons from SA and ADSA show a number of changes: the relative intensity of bands around $1710\,\text{cm}^{-1}$, $1570\,\text{cm}^{-1}$ and $1450\,\text{cm}^{-1}$ shows a decrease compared to that at 400 °C, a sign of the decomposition or removal of carbonyl-containing groups and hydroxyl-containing groups; the relative intensity increase of band at $1170\,\text{cm}^{-1}$, the appearance of a new band around $1040\,\text{cm}^{-1}$

of which the relative intensity increases with activation temperature for ADSA. The peak at $1040\,\text{cm}^{-1}$ could be due to P^+–O^- in acid phosphate esters and to the stretching vibrations in polyphosphate chain P–O–P [28]. This indicates that at least some of the formed carbon–oxygen groups decomposed at high temperatures accompanying the increase of phosphorus-containing groups.

Compared with SA (Fig. 4a), for carbons from ADSA, the relative intensities of the bands around $500\,\text{cm}^{-1}$, $1040\,\text{cm}^{-1}$ and $1170\,\text{cm}^{-1}$ displayed a trend of increase with the change of activation temperature from 400 to 700 °C (Fig. 4b). This indicates that further increase in the activation temperature has an apparent impact on the formation of phosphorus-containing groups of activated carbons from ADSA, while that of SA is not obvious. Thus, the FTIR spectra of carbons prepared with different activation temperatures indicate that higher activation temperature is preferable for the formation of phosphorus-containing groups, especially for carbons from ADSA.

3.3. Adsorption results

3.3.1. Cadmium (II) adsorption isotherms

The adsorption isotherms obtained at 25 °C for cadmium (II) with the prepared activated carbons are shown in Fig. 5. The differences observed on the adsorption capacities of these carbons cannot be explained from their different BET surface areas. The

adsorption capacity of ADSA-1-700 was greater than SA-1-400 despite the reduction in surface area of the former. Moreover, the SA-1-400 sample, which has the highest BET surface area, yields the lowest capacity. This may indicate that cadmium (II) adsorption is related to the chemistry of the carbon surface rather than the morphological properties.

It seems that relatively higher activation temperature is more efficient in producing sorbents with high potentiality for heavy metal adsorption. The observed increase in the uptake capacity of activated carbons by increasing the activation temperature of the samples activated within 400–700 °C could be attributed to the possible increase in the amount of PO_4^{3-} that may formed and retained on their surfaces [29]. The shapes of the isotherms (Fig. 5a) suggest that for the sample SA-1-700, and to a lesser extent for sample SA-1-600, there are high energy adsorption sites that lead to strong adsorption at low equilibrium concentrations. In addition, the cadmium (II) adsorption capacity of carbons from ADSA is much lower than SA. This indicated that the biopolymer composition of precursors has an essential influence on the adsorption capacity for removal of cadmium (II).

The relative adsorption capacity of the carbons prepared from SA and ADSA at different impregnation ratios are shown in Fig. 5b. It is obvious that high impregnation has an adverse effect on the cadmium (II) adsorption capacity of the activated carbons. This can be explained with the lower active centers contribute in cadmium (II) adsorption with higher impregnation ratio. As impregnation ratio increases, more phosphoric acid is incorporated into the skeleton of the precursor, and the active centers on the surface of carbons are likely to increase.

To understand the adsorption patterns, the experimental results were fitted with three popular adsorption models: Langmuir, Freundlich and Dubinin–Radushkevich models. Isotherm equations are given in Table 2, the values of the parameters and the correlation coefficients are listed in Table 3.

It is well known that the Langmuir model is usually used with an ideal assumption of a monolayer adsorption surface; the Freundlich model is usually derived to model the multilayer adsorption and for the adsorption on heterogeneous surface. The correlation coefficients (R^2) (Table 3) show that both the Freundlich and the Langmuir models can be used to fit the data and estimate model parameters, but the overall data are better fitted by Langmuir isotherm in describing the adsorption of cadmium (II) onto activated carbons. It is revealed that the energy distribution for the adsorption sites on activated carbons was of essentially a uniform type, rather than of the exponential type. Furthermore, the values of Freundlich constant n were found to be greater than 1 for all samples, indicating a favorable adsorption [30]. As to the values of q_m, they increased with the increase of the activation temper-

Table 2
Isotherm models adopted in this work and their parameters.

Isotherms	Equations	Parameters
Langmuir	$C_e/q_e = C_e/q_m + 1/(q_m K)$	q_e: equilibrium adsorption capacity (mg/g) C_e: equilibrium liquid phase concentration (mg/L) q_m: the maximum adsorption capacity (mg/g) K: constant of Langmuir (L/mg)
Freundlich	$\log q_e = \log K_F + 1/n \log C_e$	K_F: the Freundlich constant for a heterogeneous adsorbent (L/mg) $1/n$: the heterogeneity factor
Dubinin–Radushkevich	$\ln q_e = \ln q_m - k\varepsilon^2$ $\varepsilon = [RT\ln(1 + (1/C_e))]$ $E = (2k)^{-0.5}$	k: constant related to the adsorption energy (mol²/kJ²) ε: Polanyi potential R: the gas constant (kJ/mol K) T: absolute temperature (K) E: mean free energy of adsorption (kJ/mol)

ature from 400 to 700 °C. From Table 2, the maximum adsorption capacity of cadmium (II) onto SA-1-700 was more than 47 mg/g. The adsorption capacities of cadmium (II) on other adsorbents such as ADSA-1-700, SA-3-500, and ADSA-1-400 were found to be 38.91, 13.09 and 9.28 mg/g, respectively. When compared to these adsorbents, SA-1-700 had the largest capacity for the removal of cadmium (II). In additional, we compared maximum adsorption capacities obtained in this study with some other adsorbents listed in Table 4. It was suggested that SA-1-700 was an effective adsorbent for the purification of wastewater containing cadmium (II).

Langmuir and Freundlich isotherms do not give any idea about the adsorption mechanism. Dubinin–Radushkevich (D–R) isotherm describes adsorption on a single type of uniform pores. In this respect, it is more general than Langmuir and Freundlich isotherms because it assumes that only a small fraction of the surface is uniform in structure and energetically homogeneous while those of Langmuir and Freundlich are based on complete homogeneity of the entire surface which is an over-simplification. E (mean free energy of adsorption) (Table 2) is useful for estimating the type of adsorption process. If its values are between 8 and 16 kJ/mol, the adsorption process can be explained by ion exchange [36].

Table 3
Isotherms fitting parameters (25 °C).

Adsorbent	Langmuir			Freundlich			D–R			
	q_m	K	R^2	K_F	n	R^2	q_m	k	E	R^2
SA-1-400	12.36	0.09	0.8892	3.32	3.76	0.7867	9.41	0.0088	7.53	0.5859
SA-1-500	28.74	0.82	0.9968	12.69	4.17	0.9645	28.87	0.0048	10.22	0.9943
SA-1-600	40.73	1.25	0.9991	17.42	4.25	0.8525	43.31	0.0052	9.80	0.9591
SA-1-700	47.85	0.95	0.9984	20.49	4.24	0.8311	49.83	0.0049	10.13	0.9218
SA-0.5-500	22.08	0.36	0.9819	9.36	4.70	0.9915	19.83	0.0045	10.59	0.9421
SA-2-500	22.40	0.34	0.9773	9.12	4.44	0.9870	20.38	0.0050	10.04	0.9556
SA-3-500	13.09	0.13	0.9723	3.83	3.73	0.9310	10.85	0.0083	7.78	0.7676
ADSA-1-400	9.28	0.14	0.9937	2.54	3.43	0.9367	8.95	0.0129	6.22	0.9681
ADSA-1-500	18.52	0.21	0.9944	6.13	3.97	0.9845	16.78	0.0077	8.07	0.9409
ADSA-1-600	28.57	0.46	0.9977	11.16	4.15	0.9796	27.04	0.0053	9.76	0.9575
ADSA-1-700	38.91	0.72	0.9979	17.30	4.54	0.9888	35.98	0.0037	11.69	0.9612
ADSA-0.5-500	22.22	0.05	0.9617	2.30	2.09	0.9817	16.86	0.0187	5.17	0.9023
ADSA-2-500	14.64	0.53	0.9988	7.00	5.22	0.8993	14.61	0.0056	9.43	0.9618
ADSA-3-500	12.45	0.07	0.9863	1.89	2.52	0.9549	10.29	0.0169	5.44	0.8705

Table 4
Adsorption capacities for cadmium (II) using different low-cost adsorbents.

Adsorbent	Adsorption capacity (mg/g)	Reference
Olive stone carbon	1.851	[1]
Phaseolus aureus hull carbon	15.7	[31]
Ceiba pentandra hull carbon	19.5	[32]
Jordanian olive cake carbon	21	[33]
Apricot stone carbon	33.57	[34]
Bagasse carbon	38.03	[35]
SA-1-700	47.85	Present study

In this study, E values of the activated carbons fall within a relatively wide range of 5.17–11.69 kJ/mol (Table 3). Therefore, the main adsorption mechanism of cadmium (II) on activated carbons prepared from different precursors at various activation conditions could be different. An ion-exchange process alone does not appear sufficient to understand the trend observed on the adsorption capacities for all of the adsorbents. These results indicate that other types of interactions, besides ion exchange, must be established in the adsorption of cadmium (II). Among the earlier efforts, Sánchez-Polo and Rivera-Utrilla [37] found that electrostatic interactions also play an important role in the mechanism of cadmium (II) adsorption, especially on acidic carbons.
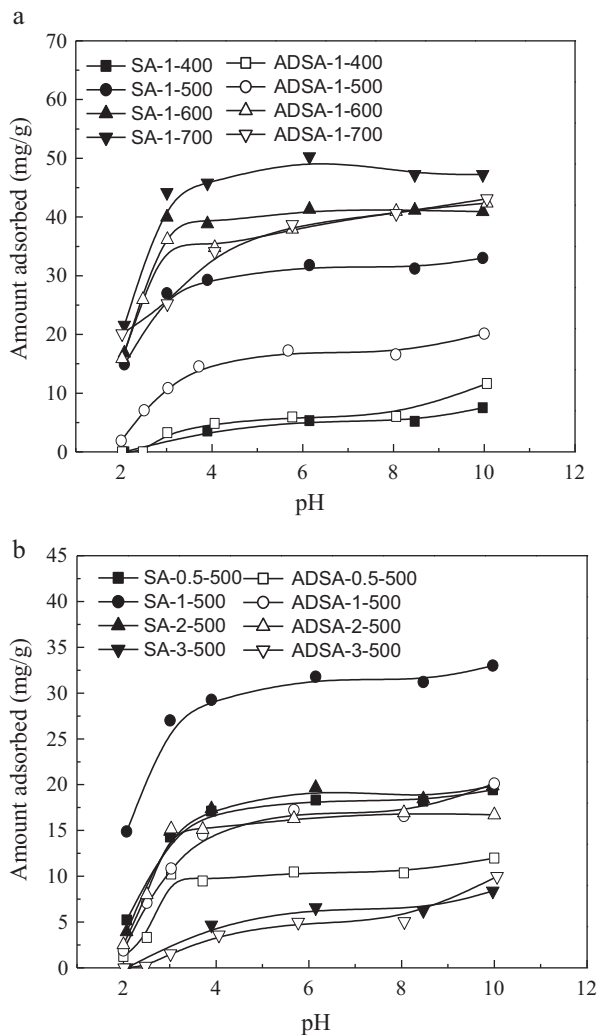

Fig. 6. Effect of the pH on the removal of cadmium (II) onto carbons prepared from SA and ADSA at different activation temperatures (a) and different impregnation ratios (b).

3.3.2. The effect of pH on adsorption process

The pH of a solution is one of the parameters with the greatest influence on the adsorption of metal ions by activated carbon. To investigate its effect on cadmium (II) adsorption, experiments were conducted with pH ranging from 2 to 10. The results obtained for adsorbents are shown in Fig. 6. It is obvious from the figure that at pH 2, the amount of cadmium (II) adsorbed on the activated carbons was very low, possibly because of the high concentration of protons in solution that restricts the exchange between the cadmium (II) species and the protons on the carbon surface [38]. In addition, when the solution pH was around 2, the net charge on the surface of activated carbons was positive since the pH_{PZC} was found to be 2.50–3.25. At $pH < pH_{PZC}$, the positively charged cadmium species may be repelled by the positively charged carbon surface molecules and results in a low cadmium (II) equilibrium adsorption capacity cadmium (II) [39]. With the increase of solution pH, the H^+ on the surface sites and positive surface charge of activated carbons decreased. Hence, the electrostatic repulsions decreased rapidly with the solution pH increasing from 2 to 4, which caused the increase of cadmium (II) adsorption amount. When the solution pH was higher than 4, the surface of activated carbons was negatively charged. As a result, electrostatic attractions between the adsorbent and the cadmium (II) occurred. It is evidently that the carbon is effective for the maximum removal of cadmium (II) over the pH range 4–8. At pH > 8 precipitation of cadmium (II) may take place and continues to increase with further increase of pH.

4. Conclusions

The activated carbon prepared from *S. alterniflora* is identified to be an effective adsorbent for the removal of cadmium (II) from aqueous solutions, while carbons prepared from ADSA show lower wastewater treatment potential. Both the composition of lignocellulosic precursor and the activation conditions have an important effect on the activated carbon products in terms of physicochemical properties and adsorption capacities. An impregnation ratio and an activation temperature around 1.0 and 700 °C, respectively, are recommended as the best combination of operating conditions to prepare activated carbons for cadmium (II) adsorption. Adsorption results fit better with Langmuir isotherm which shows the homogeneous characteristics of the adsorption sites on activated carbons.

References

[1] I. Kula, M. Ugurlu, H. Karaoglu, A. Çelik, Adsorption of Cd(II) ions from aqueous solutions using activated carbon prepared from olive stone by ZnCl2 activation, Bioresource Technology 99 (2008) 492–501.
[2] M.A.A. Zaini, R. Okayama, M. Machida, Adsorption of aqueous metal ions on cattle-manure-compost based activated carbons, Journal of Hazardous Materials 170 (2009) 1119–1124.
[3] A.M. Puziy, O.I. Poddubnaya, A. Martínez-Alonso, A. Castro-Muñiz, F. Suárez-García, J.M.D. Tascón, Oxygen and phosphorus enriched carbons from lignocellulosic material, Carbon 45 (2007) 1941–1950.
[4] R. Yavuz, H. Akyildiz, N. Karatepe, E. Çetinkaya, Influence of preparation conditions on porous structures of olive stone activated by H_3PO_4, Fuel Processing Technology 91 (2010) 80–87.
[5] J. de Celis, N.E. Amadeo, A.L. Cukierman, In situ modification of activated carbons developed from a native invasive wood on removal of trace toxic metals from wastewater, Journal of Hazardous Materials 161 (2009) 217–223.
[6] Y. Guo, D.A. Rockstraw, Activated carbons prepared from rice hull by one-step phosphoric acid activation, Microporous and Mesoporous Materials 100 (2007) 12–19.

[7] Ö. Gerçel, H.F. Gerçel, Adsorption of lead(II) ions from aqueous solutions by activated carbon prepared from biomass plant material of Euphorbia rigida, Chemical Engineering Journal 132 (2007) 289–297.

[8] S. Chen, J. Zhang, C. Zhang, Q. Yue, Y. Li, C. Li, Equilibrium and kinetic studies of methyl orange and methyl violet adsorption on activated carbon derived from Phragmites australis, Desalination 252 (2010) 149–156.

[9] C.-H. Chung, Forty years of ecological engineering with Spartina plantations in China, Ecological Engineering 27 (2006) 49–57.

[10] R.S. Zhang, Y.M. Shen, L.Y. Lu, S.G. Yan, Y.H. Wang, J.L. Li, Z.L. Zhang, Formation of Spartina alterniflora salt marshes on the coast of Jiangsu Province, China, Ecological Engineering 23 (2004) 95–105.

[11] H. Li, L. Zhang, An experimental study on physical controls of an exotic plant Spartina alterniflora in Shanghai, China, Ecological Engineering 32 (2008) 11–21.

[12] C. Zhou, S. An, Z. Deng, D. Yin, Y. Zhi, Z. Sun, H. Zhao, L. Zhou, C. Fang, C. Qian, Sulfur storage changed by exotic Spartina alterniflora in coastal saltmarshes of China, Ecological Engineering 35 (2009) 536–543.

[13] R. Wang, L. Yuan, L. Zhang, Impacts of Spartina alterniflora invasion on the benthic communities of salt marshes in the Yangtze Estuary, China, Ecological Engineering 36 (2010) 799–806.

[14] S. Yang, J. Li, Z. Zheng, Z. Meng, Characterization of Spartina alterniflora as feedstock for anaerobic digestion, Biomass and Bioenergy 33 (2009) 597–602.

[15] P. Qin, M. Xie, Y. Jiang, Spartina green food ecological engineering, Ecological Engineering 11 (1998) 147–156.

[16] G. Chen, Z. Zheng, S. Yang, C. Fang, X. Zou, J. Zhang, Improving conversion of Spartina alterniflora into biogas by co-digestion with cow feces, Fuel Processing Technology 91 (2010) 1416–1421.

[17] S. Brunauer, P.H. Emmett, E. Teller, Adsorption of gases in multimolecular layers, Journal of the American Chemical Society 60 (1938) 309–319.

[18] B.C. Lippens, J.H. de Boer, Studies on pore systems in catalysts: V. The t method, Journal of Catalysis 4 (1965) 319–323.

[19] S.K. Milonjic, A.L. Ruvarac, M.V. Susic, The heat of immersion of natural magnetite in aqueous solutions, Thermochimica Acta 11 (1975) 261–266.

[20] S. Yang, J. Li, Z. Zheng, Z. Meng, Lignocellulosic structural changes of Spartina alterniflora after anaerobic mono- and co-digestion, International Biodeterioration & Biodegradation 63 (2009) 569–575.

[21] Suhas, P.J.M. Carrott, M.M.L. Ribeiro Carrott, Lignin – from natural adsorbent to activated carbon: a review, Bioresource Technology 98 (2007) 2301–2312.

[22] B. Cagnon, X. Py, A. Guillot, F. Stoeckli, G. Chambat, Contributions of hemicellulose, cellulose and lignin to the mass and the porous properties of chars and steam activated carbons from various lignocellulosic precursors, Bioresource Technology 100 (2009) 292–298.

[23] Y. Guo, D.A. Rockstraw, Physical and chemical properties of carbons synthesized from xylan, cellulose, and Kraft lignin by H_3PO_4 activation, Carbon 44 (2006) 1464–1475.

[24] A. Reffas, V. Bernardet, B. David, L. Reinert, M.B. Lehocine, M. Dubois, N. Batisse, L. Duclaux, Carbons prepared from coffee grounds by H_3PO_4 activation: charac-
terization and adsorption of methylene blue and Nylosan Red N-2RBL, Journal of Hazardous Materials 175 (2010) 779–788.

[25] A.M. Puziy, O.I. Poddubnaya, A. Martínez-Alonso, F. Suárez-García, J.M.D. Tascón, Surface chemistry of phosphorus-containing carbons of lignocellulosic origin, Carbon 43 (2005) 2857–2868.

[26] A. Klijanienko, E. Lorenc-Grabowska, G. Gryglewicz, Development of mesoporosity during phosphoric acid activation of wood in steam atmosphere, Bioresource Technology 99 (2008) 7208–7214.

[27] A. Kriaa, N. Hamdi, E. Srasra, Removal of Cu (II) from water pollutant with Tunisian activated lignin prepared by phosphoric acid activation, Desalination 250 (2010) 179–187.

[28] T.-H. Liou, Development of mesoporous structure and high adsorption capacity of biomass-based activated carbon by phosphoric acid and zinc chloride activation, Chemical Engineering Journal 158 (2010) 129–142.

[29] A.-N.A. El-Hendawy, The role of surface chemistry and solution pH on the removal of Pb^{2+} and Cd^{2+} ions via effective adsorbents from low-cost biomass, Journal of Hazardous Materials 167 (2009) 260–267.

[30] A. Fouladi Tajar, T. Kaghazchi, M. Soleimani, Adsorption of cadmium from aqueous solutions on sulfurized activated carbon prepared from nut shells, Journal of Hazardous Materials 165 (2009) 1159–1164.

[31] M.M. Rao, D.K. Ramana, K. Seshaiah, M.C. Wang, S.W.C. Chien, Removal of some metal ions by activated carbon prepared from Phaseolus aureus hulls, Journal of Hazardous Materials 166 (2009) 1006–1013.

[32] M. Madhava Rao, A. Ramesh, G. Purna Chandra Rao, K. Seshaiah, Removal of copper and cadmium from the aqueous solutions by activated carbon derived from Ceiba pentandra hulls, Journal of Hazardous Materials 129 (2006) 123–129.

[33] I.H. Aljundi, N. Jarrah, A study of characteristics of activated carbon produced from Jordanian olive cake, Journal of Analytical and Applied Pyrolysis 81 (2008) 33–36.

[34] M. Kobya, E. Demirbas, E. Senturk, M. Ince, Adsorption of heavy metal ions from aqueous solutions by activated carbon prepared from apricot stone, Bioresource Technology 96 (2005) 1518–1521.

[35] D. Mohan, K.P. Singh, Single-multi-component adsorption of cadmium and zinc using activated carbon derived from bagasse – an agricultural waste, Water Research 36 (2002) 2304–2318.

[36] A. Kilislioglu, B. Bilgin, Thermodynamic and kinetic investigations of uranium adsorption on amberlite IR-118H resin, Applied Radiation and Isotopes 58 (2003) 155–160.

[37] M. Sánchez-Polo, J. Rivera-Utrilla, Adsorbent–adsorbate interactions in the adsorption of Cd(II) and Hg(II) on ozonized activated carbons, Environmental Science & Technology 36 (2002) 3850–3854.

[38] G. Blázquez, F. Hernáinz, M. Calero, L.F. Ruiz-Núñez, Removal of cadmium ions with olive stones: the effect of somes parameters, Process Biochemistry 40 (2005) 2649–2654.

[39] K. Li, Z. Zheng, Y. Li, Characterization and lead adsorption properties of activated carbons prepared from cotton stalk by one-step H_3PO_4 activation, Journal of Hazardous Materials 181 (2010) 440–447.